Processing Bistatic Radar Observations of Comet 67P/Churyumov-Gerasimenko

G.G. Peytaví[1], T.P. Andert[1], S. Remus[2], R.A. Simpson[3], M.Pätzold[4], B. Häusler[1], S. Tellmann[3], M.K. Bird[4]

[1]Institute of Space Technology & Space Applications (ISTA), Universität der Bundeswehr München, Munich, Germany
[2]Telespazio VEGA UK LTD, SRE-OO, ESTEC, Noordwijk, The Netherlands
[3]Department of Electrical Engineering, Stanford University, California, USA
[4]Rheinisches Institut für Umweltforschungs (RIU), Department of Planetary Research at the University of Cologne, Köln, Germany

Introduction

Objectives of the Rosetta Radio Science investigations included determining the dielectric properties, small-scale roughness, and rotational state of the nucleus of comet 67P/Churyumov-Gerasimenko (67P/C-G) from bistatic radar (BSR) measurements. The radio transmitter and high gain antenna (HGA) on the spacecraft beamed right circularly polarized (RCP) radio signals at two wavelengths - 3.6 cm (X-Band) and 13 cm (S-Band) - toward the nucleus surface. Parts of the impinging radiation was then scattered toward a ground station of the DSN on Earth, where it was received and recorded coherently in both RCP and left circular polarization (LCP). Between late September and mid-December 2014, six BSR experiments were conducted successfully at 67P/CG. In-phase and quadrature samples were collected at sampling rates of 25 KHz and 1 KHz.

For a specular reflection point illuminated under an incidence angle α smaller than the Brewster limit of the surface material, the ratio of the reflected power in the same incident polarization ρ_R to opposite polarization ρ_L yields a parametric relation to the surface dielectric constant ε.

$$\rho_R = 0.25\,(R_v + R_H)^2 \qquad R_H = \frac{\cos\alpha - \sqrt{\varepsilon - \sin^2\alpha}}{\cos\alpha + \sqrt{\varepsilon - \sin^2\alpha}}$$

$$\rho_L = 0.25\,(R_v - R_H)^2 \qquad R_V = \frac{\varepsilon\cos\alpha - \sqrt{\varepsilon - \sin^2\alpha}}{\varepsilon\cos\alpha + \sqrt{\varepsilon - \sin^2\alpha}}$$

(Simpson et al., 2011)

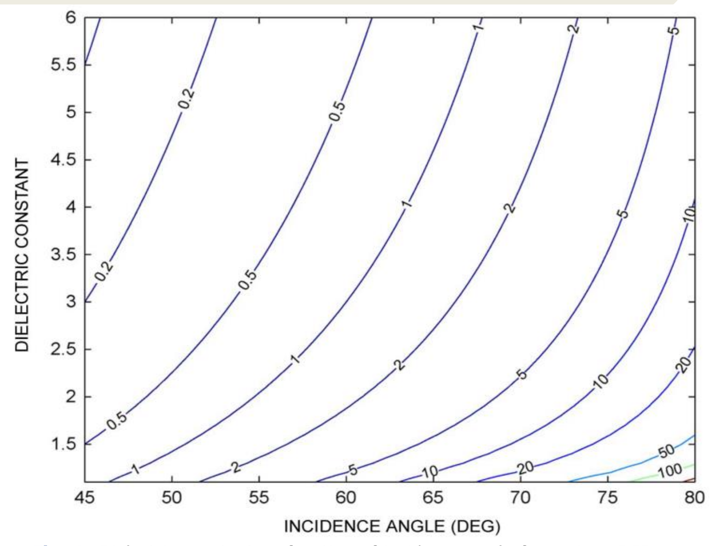

Fig. 1: Dielectric constant as function of incidence angle for various RCP to LCP power ratios (Simpson et al., 2011).

Experiment phase	Acronym
Ambient load	AMB
Ambient load + noise diode	AMB + ND
DSN in sky pointing	SKY
Spacecraft carrier tracking	BCAL
DSN in planetary pointing. The system noise temperature can be determined at this point.	MINICAL
Bi-static radar observations of the surface	BSR

Tab. 1: BSR experiment measurement phases.

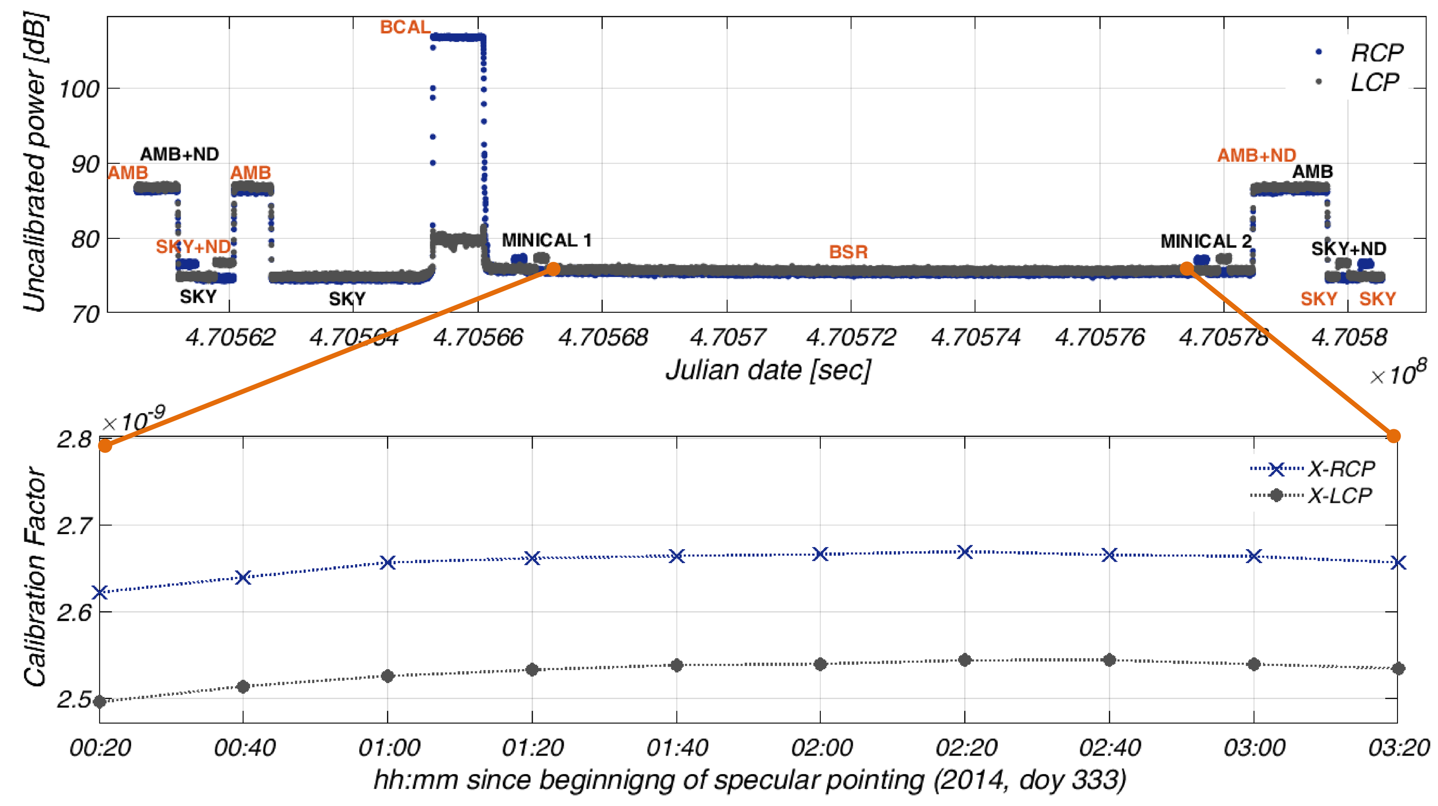

Fig. 2: (Top) Averaged spectral power of the 1KHz **X-RCP** and **X-LCP** complex voltage samples as function of time. Power variations are indicative of the various experiment calibration phases.
(Bottom) Noise floor calibration factors for **X-RCP** and **X-LCP** channels. Factors are reconstructed from the system noise temperature during pre-cal and post-cal data, and through comparison with the uncalibrated noise floor during surface observation.

The BSR experiment timeline proposed by (Simpson et al., 2011) includes pre-calibration and post-calibration procedures to evaluate the system noise temperature on each data channel. This procedure involves various phases during which the behaviour of the system is recorded under different loads. Using these recordings, a power conversion factor can be obtained to calibrate the echo signal power in post processing.

Geometric Analysis

1. Is the area illuminated by the HGA statistically specular?

- **Obtain a model of the HGA footprint** as the surface intersection of a mesh antenna beam model and mesh comet model (X-band HGA main lobe half-width @3dB = 0.48 deg).
- **Divide the footprint in triangular facets** (independent from model resolution)
- For each facet of the footprint, **obtain centroid coordinates and surface normal vector**
- Given Tx and Rx locations, **calculate $\alpha_i, \alpha_r, \alpha_a$** for each centroid and for the HGA boresight direction
- **Calculate mean angles** for for overall footprint

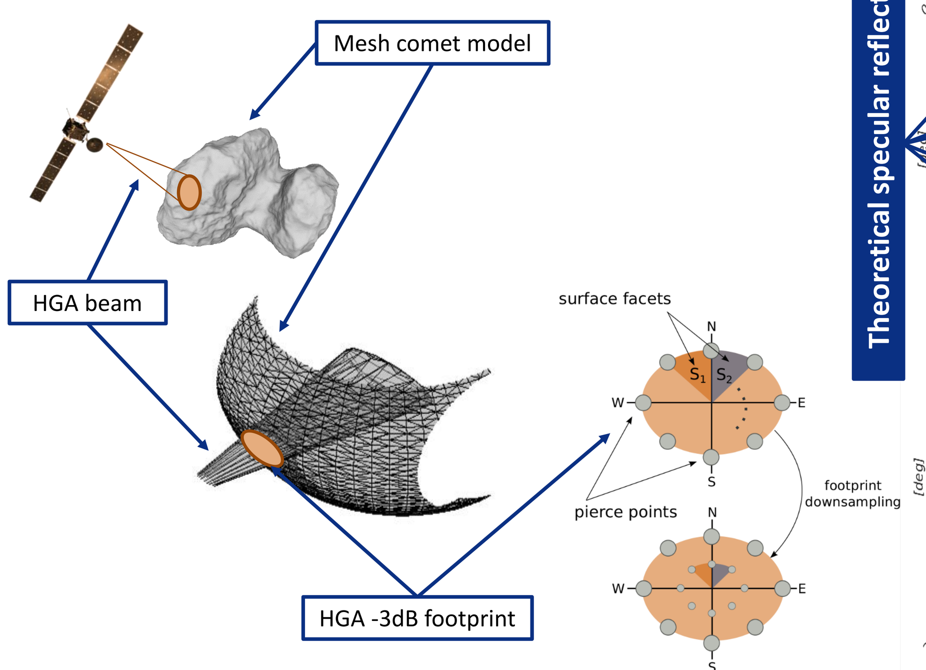

Fig. 3: Schematic representation of the numerical procedure to obtain the antenna footprint reflection geometry at a particular epoch. The footprint is divided in triangular facets, which are the result of interpolating surface slopes of smaller facets of available comet shape models.

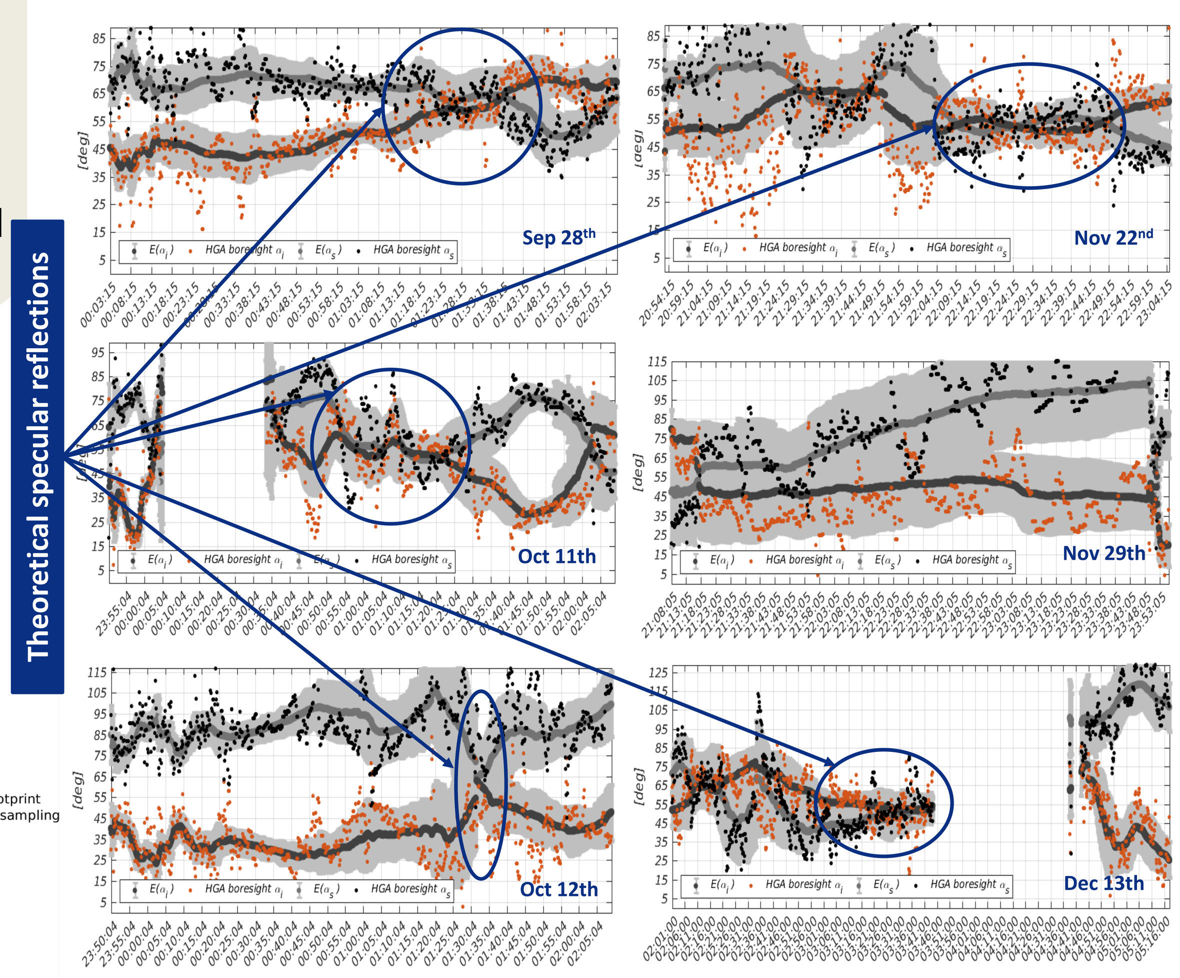

Fig. 4: Expected surface **incidence** (orange dots) and **reflection** (black dots) angles for the high-gain antenna (HGA) boresight direction. The **mean and standard deviation** (1σ) of the same angles, computed for the half-power HGA beamwidth footprint on the surface of the comet, are represented as background gray areas. A facet grid of 1 deg in azimuth and 0.05 deg in off-boresight angle were used to represent the footprint topography at each epoch.

2. Are there single specular points/regions within the footprint?

- For each facet centroid, check specular conditions:
  a) Co-planarity: $V_p = |\mathbf{n} \cdot (\mathbf{t} \times \mathbf{r})| \approx 0$
  b) Law of reflection: $\alpha_i = \alpha_r \rightarrow \widehat{tn} = \widehat{nr}$

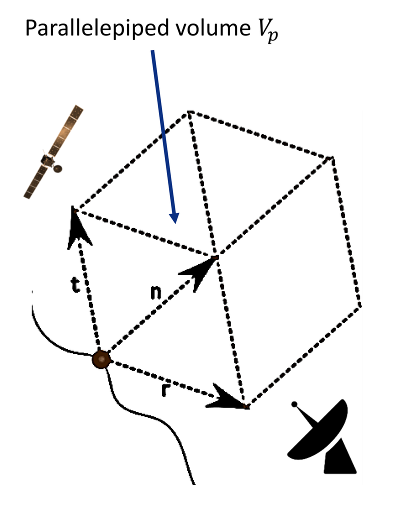

Fig. 5: Schematic of the reflection geometry vectors: surface to transmitter t, surface to receiver r and surface normal n at the location of the specular point.

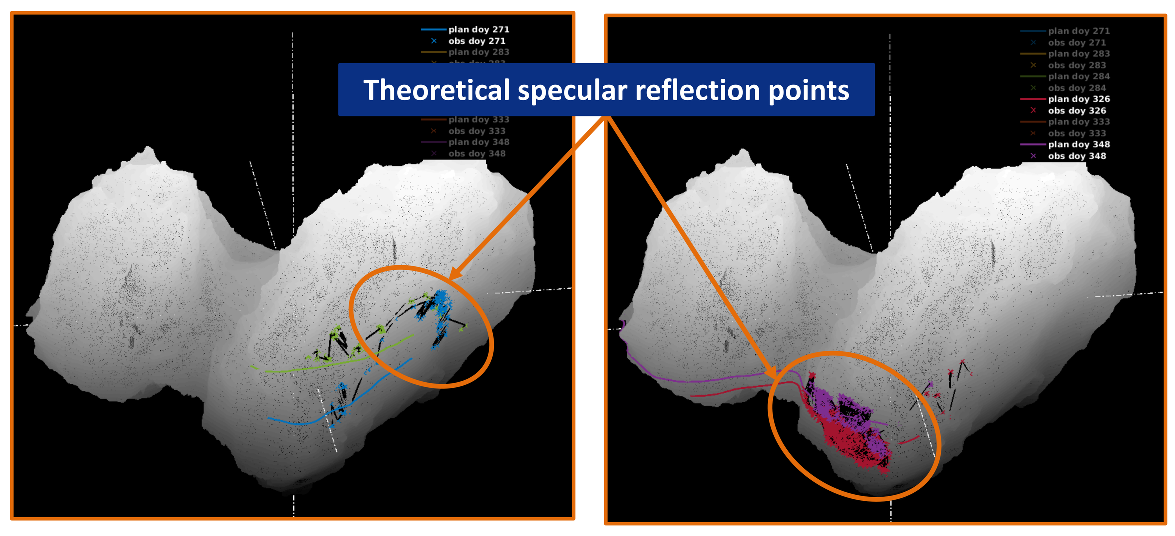

Fig. 6: Predicted locations (continuous lines) and updated locations (crosses) of the specular reflection points on the comet surface. Predicted locations were computed during experiment planning on a triaxial ellipsoid. Update locations are computed on the latest available facet shape model (Preusker et al., 2017). Represented datasets are for **doy 271**, **doy 284**, **doy 326**, and **doy 348**.

3. What is the theoretical frequency response of the illuminated area?

- **Differential Doppler** Direct Signal – Echo Signal: $\Delta f = f_d - f_s$
- **Spectral dispersion** of the echo signal:

$$B = \frac{4\sqrt{\ln 2}\, v_{sp}\, \varsigma}{\lambda} \cos\theta$$

(Simpson, 1993)

Date	doy	DSN	Δf (Hz)	B (Hz)	ς (deg)	α_i (deg)
SEP 29	271	DSS-14	1.40-1.73	0.16	13.12	55.44
OCT 11	283	DSS-14	5.65-6.04	0.47	17.00	49.21
OCT 12	284	DSS-14	1.11-3.76	0.72	18.59	58.69
NOV 22	326	DSS-14	1.73-2.09	0.51	17.36	51.81
NOV 29	333	DSS-14	0.79-3.52	0.24	32.65	41.37
DEC 14	348	DSS-43	0.95-1.27	1.10	21.21	48.78

Tab. 2: Expected values for the differential Doppler frequency shift Δf between direct signal and echo, echo spectral dispersion B, surface RMS slope ζ, and specular reflection angle α_i.

RSI BSR Signal Processing

1. Spectral estimation scheme

Based on the geometric analysis, BSR echo signals from the surface of 67P/C-G are expected: (a) **spectrally adjacent** to the direct signal (from a fraction of a Hz to few Hz), (b) **weak** in amplitude (overlapping in frequency with additional clutter noise from non-specular regions), and (c) **narrow band** (spread roughly over 1 Hz). It is hence necessary to adapt conventional BSR processing schemes to the specific observation geometry at the comet.

The specular point traversed slowly on the comet surface $(0.52 \pm 0.3)\ m/s$ during the measurements. The spacecraft travelled at a comparable rate relative to the comet $(1.88 \pm 0.85)\ m/s$. Both the direct and echo signals drifted very slow gently in frequency over time. A significantly large signal integration time window can be employed to reduce noise variance in the data. Integration windows up to 10 min in duration (~1.5 mHz spectral resolution) have been used for this work.

We selected a moving window average procedure, also known as the **non-parametric Welch's periodogram** (See e.g., Kay, 1988). This approach reduces the bias of the estimate by overlapping consecutive averaging windows. This procedure has been successfully applied for the computation of uncalibrated spectral echo power from the surface of 67P/C-G.

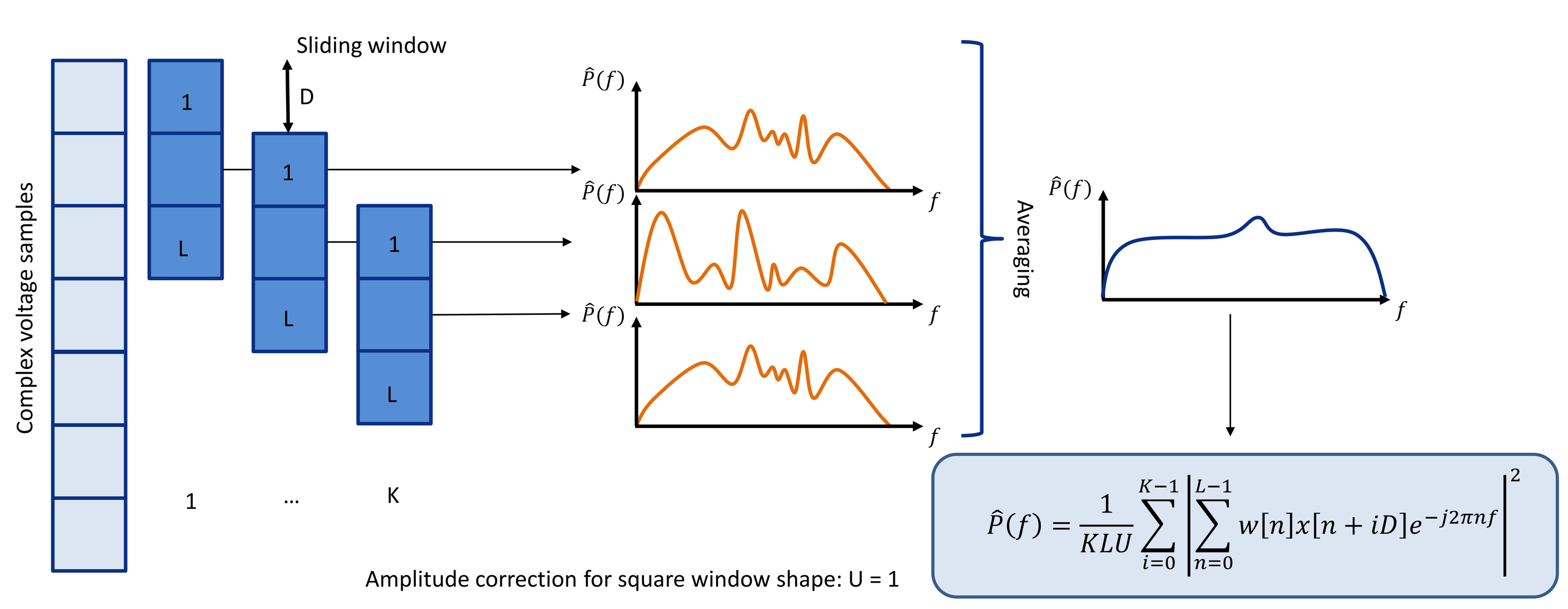

$$\hat{P}(f) = \frac{1}{KLU} \sum_{i=0}^{K-1} \left| \sum_{n=0}^{L-1} w[n]x[n+iD]e^{-j2\pi nf} \right|^2$$

Fig. 7: Schematic of the average periodogram estimation technique with overlapping sliding window.

2. ROS BSR signal processing pipeline

In the datasets collected for the Rosetta RSI BSR experiments, echo signal tones are visible in the X-RCP and X-LCP channels on both, 1KHz and 25 KHz logs. The diagram below depicts the proposed processing pipeline to reconstruct echo signal power from the surface of comet 67P/C-G. The data presented here corresponds to the 25 KHz records for doy 333 in 2014. These measurements were conducted over the north neck region of the comet, close to the body spin axis. For these dataset, the geometry analysis indicated potential specular reflection points at an angle of ~41 deg.

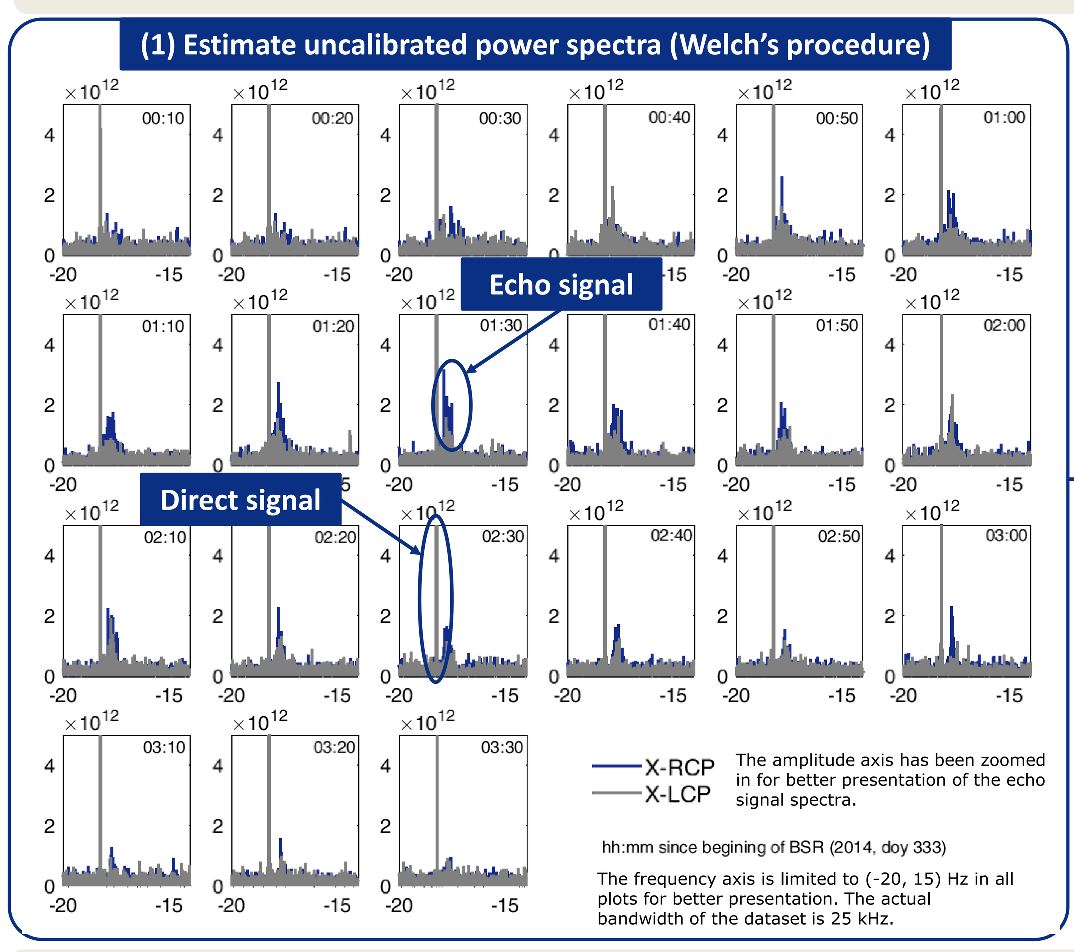

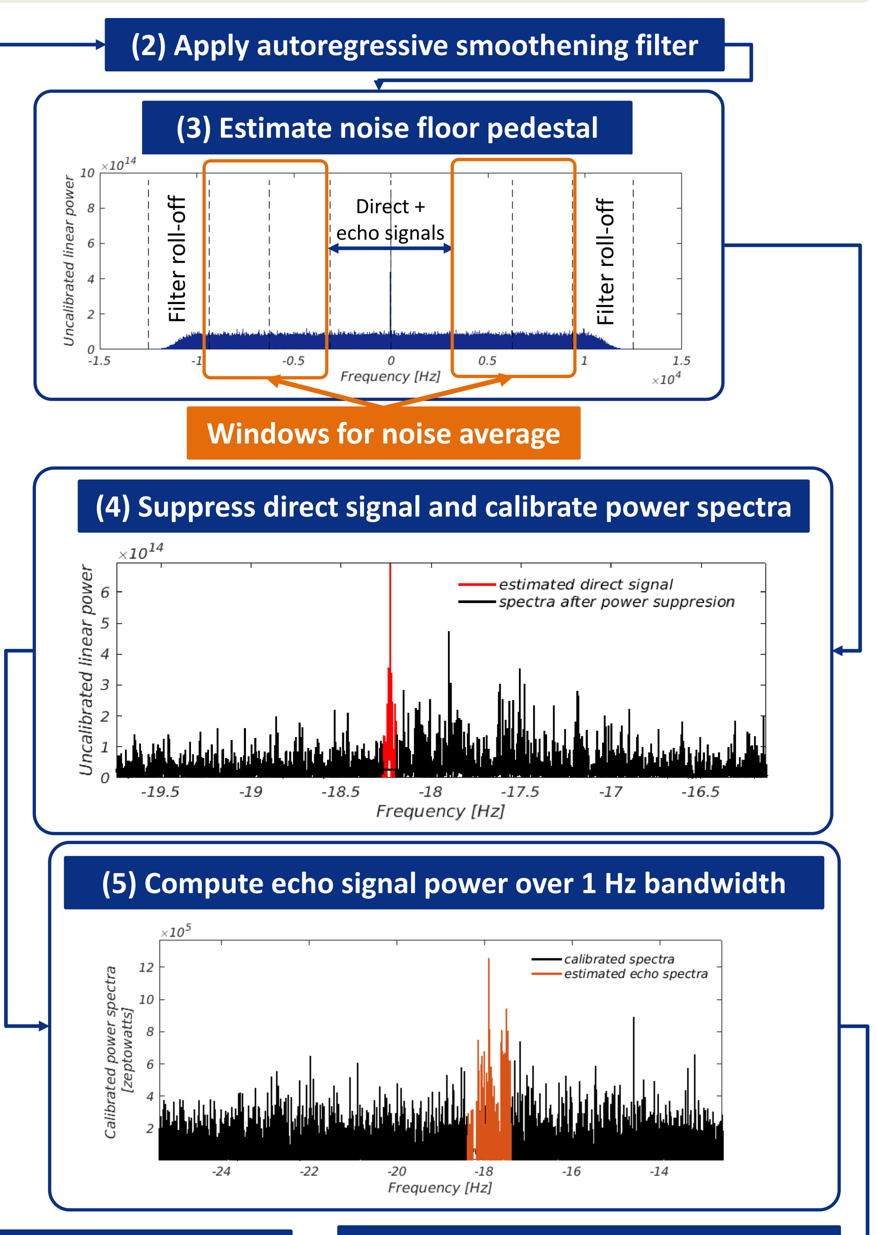

X-RCP to X-LCP power ratios on doy 333 average to 1.37 ± 0.33. For a specular reflection angle $\alpha_i \approx 41\,deg$, the computed ratios yield a non-physical dielectric constant $(\varepsilon < 1)$. It is believed that a partial specular reflection is occluded by additional clutter echoes close to the Brewster limit, hence the strong RCP component. A more accurate physical reflection model is therefore necessary.

(7) Constrain dielectric constant

Rosetta Science Workshop and SWT 49
May 28th -June 1st 2018, Rhodes, Greece

Acknowledgement
The Rosetta Radio Science Investigation (RSI) experiment is funded by Deutsches Zentrum für Luft- und Raumfahrt, Bonn-Oberkassel, under grant 50QM1004 and 50QM1005.
Supported by: Federal Ministry for Economic Affairs and Energy on the basis of a decision by the German Bundestag